QUANTUM CONFINEMENT IN NANOCRYSTALLINE SILICON

M. L. Ciurea[*]

National Institute of Materials Physics, P.O. Box MG-7, Bucharest-Magurele 77125, Romania

Quantum confinement effects in different kinds of nanocrystalline silicon systems are experimentally and theoretically investigated. Porous silicon structured as a nanowire network and silicon nanodots embedded in amorphous silicon dioxide are studied. The main quantum confinement effect in both cases is represented by the appearance of new energy levels in the silicon band gap. The corresponding energies can be experimentally determined from the current – temperature characteristics, which show an Arrhenius-like behavior. The curves present several activation energies between liquid nitrogen temperature and room temperature. The energy levels can be evaluated from a quantum well model. The fundamental level is located at the top of the valence band. The change of the activation energy is then related with the filling of the levels. The ratios of the consecutive activation energies in the current – temperature characteristics prove that the excitation undergoes the angular momentum conservation law imposed by the applied electric field. The estimation of the mean size of the nanocrystals from the values of the activation energies is in good agreement with the microstructure investigations performed on the samples. The confinement levels are also in good agreement with the photoluminescence measurements.

1. Introduction

Quantum confinement effects play a major role in the behavior of the nanocrystalline systems. In the case of the nanocrystalline silicon (nc-Si), quantum confinement is dominant in transport processes and has an important contribution to the optical phenomena. Carrier motion in nc-Si exhibits a variety of different behaviors, such as ballistic transport [1], tunneling (Fowler-Nordheim [2], Schottky [3], Poole-Frenkel [4, 5], or field-assisted [6, 7]), Coulomb blockade [6 – 8], and percolation [9]. Each of these features of carrier motion has attracted a great deal of interest and the quantum theory of high-field carrier transport has been developed to a high level of sophistication.

The quantum confinement determines the enlargement of the band gap [10] and leads to the breakdown of the momentum conservation rule [11], allowing no-phonon optical transitions (like in the case of a direct gap). But its main contribution consists in the appearance of new energy levels. These levels introduce new activation energies in the temperature dependence of the current (and conductivity) [12 – 16]. At the same time, these levels introduce supplementary optical transitions [11, 17].

The quantum confinement levels that appear in nc-Si systems are investigated in the present paper, both experimentally and theoretically. Two kinds of such systems were investigated, namely nanocrystalline porous silicon (nc-PS) and Si/SiO_2 nanocomposite films (nc-Si dots embedded in amorphous SiO_2). Section 2 deals with the preparation of the samples. Section 3 presents the experimental results, and Section 4 the theoretical model for the computation of the quantum

---

[*] Corresponding author: ciurea@.infim.ro

confinement levels. The experimental results are discussed in the frame of the model in Section 5, and the conclusions are stated in the last Section.

2. Preparation and measurements

The nc-PS layers were obtained by etching p-type (100) Si wafers (5 – 15 Ω·cm resistivity) in two steps [15, 18, 19]. The first step used electrochemical etching in HF (49%)-C_2H_5OH (1:1 volume ratio) under constant 5-15 mA/cm^2 current density. The second step used photochemical etching: the samples were illuminated *in situ* for 1.5 – 3 min with a Xenon lamp. After the etching, the samples were cleaned in double distilled water and dried in air for two weeks (fresh samples). The samples were then stored in ambient conditions, that induce native oxidation. The sample properties were stabilized after 1.5 years (stabilized samples). Anodic oxidation was also used to stabilize the samples.

Si/SiO_2 nanocomposite films were deposited by co-sputtering of Si and SiO_2 on rectangular quartz slides (13 cm length, 2 cm width), in a pure 19 mTorr Argon atmosphere [7]. The thickness of the films obtained after 12 h sputtering is 9 μm. The films were then annealed at 1100 °C for 30 min in a N_2 flow, in order to produce the nucleation of crystallites. This method allows the deposition in a single run of films with variable volume concentration of nc-Si from practically $x = 0$ % to practically $x = 100$ %.

The microstructure of the samples was studied by using both scanning electron microscopy (SEM) and transmission electron microscopy (TEM) with selected area electron diffraction (SAED) [7, 19, 20]. The investigations were performed with a TEMSCAN JEOL 200CX analytic electron microscope and a high resolution TOPCON 002B microscope. The cross-sectional PS specimens for TEM were prepared with M-bond glue, and a Gatan instrument with two argon ion guns at 3.5 kV was used for the ion milling. The glue was heated only after 24 h, so that it could penetrate the pores while fluid. The Si/SiO_2 specimens were prepared by scratching the layer with a thin diamond knife and collecting the small fragments with flake morphology on holey carbon grids. The local nanostructure is totally preserved by this method.

The temperature dependence of the dark current ($I – T$) between liquid nitrogen and room temperatures was investigated using a Keithley 642 electrometer, a Keithley 2000 multimeter, and an Agilent E3631A d.c. power supply. The PS samples were prepared in sandwich configuration: bottom Al / c-Si / PS / top Al. The top electrode was thermally evaporated at an angle of 15 ° with the PS layer, while the bottom one was annealed to become ohmic [15, 19]. The $I – T$ characteristics were measured in the 150 – 300 K range, at low voltages (1 – 2 V), for both bias polarities. The Si/SiO_2 samples were prepared in coplanar configuration, with 50 parallel aluminum contacts (7 mm long, 2 mm width, 2 mm distance) that allow the measuring of different nc-Si concentration regions. The characteristics were measured in the same temperature range, at both low and high voltages (1 – 5 and 25 V).

3. Experimental results

The microstructure investigations proved that our nc-PS layers present a two-level porosity. The first level is formed by a honeycomb-like system of alveolar columnar macropores (1.5 – 3 μm diameter) that cross the whole film thickness orthogonal on the film surface. The macroporosity is of about 70 %. The alveolar walls (100 – 200 nm thickness) present the second porosity level. They are formed by a nanowire network (1 – 5 nm diameter), with 50 % porosity.

The presence of nc-Si was clearly evidenced from the $x = 20$ % region of the Si/SiO_2 film, where the mean diameter of the crystallites is 3 nm [21]. The silicon crystallites appear with {111} facets if the [110] zone axis is well aligned. The mean diameter of the nanodots is here around 5 nm and they tend to form chain networks. The majority of the nanocrystallites remain under 10 nm. The bigger crystallites present lattice defects, like twins or staking faults. The amorphous silicon dioxide does not exceed 5 nm between nanodots. The SAED pattern shows some strong spots on the ring reflection, meaning that some large (15 – 20 nm) Si crystallites are present in the region.

For fresh nc-PS samples, the $I – T$ characteristic shows an Arrhenius-like behavior with one activation energy on the whole temperature range, independent on the bias polarity, as one can see in Fig. 1 (Fig. 2, Ref. 15). The activation energy value is situated in the dispersion interval 0.49 – 0.55 eV.
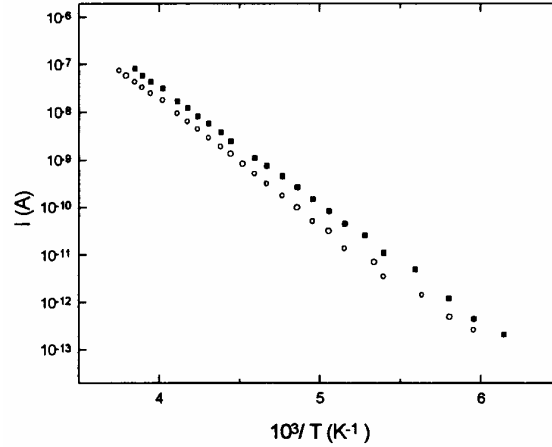
Fig. 1. $I - T$ characteristics for nc-PS fresh sample: ○ $U_a = 1$ V ('+' on c-Si),
■ $U_a = -1$ V ('+' on nc-PS) [15].

Stabilized nc-PS samples characteristics present two activation energies, as one can see from the relatively abrupt change of slope in Fig. 2 (Fig. 5, Ref. 15). The low temperature value for the activation energy is very close to that found for fresh samples, but slightly increased to 0.50 – 0.60 eV. At temperatures higher than about 280 K, a new activation energy of 1.20 – 1.80 eV appears. The ratio of the mean values of the activation energy ($E_{1m} = 0.55 \pm 0.05$ eV, $E_{2m} = 1.50 \pm 0.30$ eV) is $E_{2m}/E_{1m} = 2.73$.
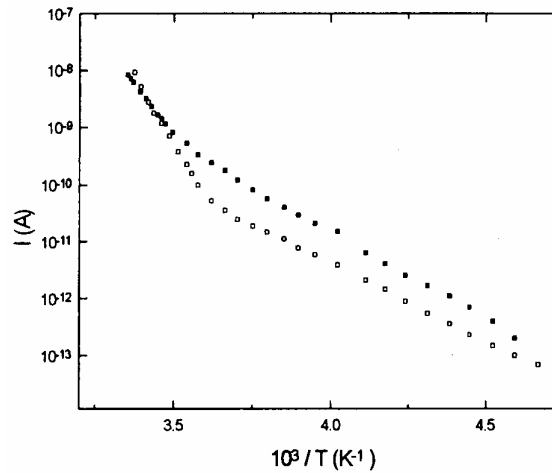

Fig. 2. $I - T$ characteristics for nc-PS stabilized sample:
■ $U_a = 2$ V ('+' on c-Si), □ $U_a = -2$ V ('+' on nc-PS) [15].

Fig. 3 presents the $I - T$ characteristics for Si/SiO$_2$ films, measured at $x = 75$ % region for two values of the applied bias, 5 and 25 V, in the temperature range 200 – 300 K [16]. The activation energy values are $E_1 = 0.29 \pm 0.01$ eV, $E_2 = 0.50 \pm 0.01$ eV for $U = 5$ V, and $E_1 = 0.31 \pm 0.01$ eV, $E_2 = 0.52 \pm 0.01$ eV for $U = 25$ V, respectively. The ratio of the mean values ($E_{1m} = 0.30 \pm 0.01$ eV, $E_{2m} = 0.51 \pm 0.01$ eV) is $E_{2m}/E_{1m} = 1.70$.

The photoluminescence measurements on fresh nc-PS samples [18] show the existence of two maxima, at 1.54 ± 0.03 eV and 1.72 ± 0.05 eV. The maximum at 1.54 eV is reduced after ageing [18], while the energy of the other one is slightly increased, up to 1.77 ± 0.05 eV. This suggests that the lower maximum is related to surface states which are diminished by oxidation, and the higher maximum is due to quantum confinement.

The investigations of Si/SiO$_2$ samples show photoluminescence at lower nc-Si concentration, where the conduction is vanishingly small [22]. The energy of the maximum is 1.70 ± 0.05 eV and it shifts to lower values as the nc-Si concentration increases.
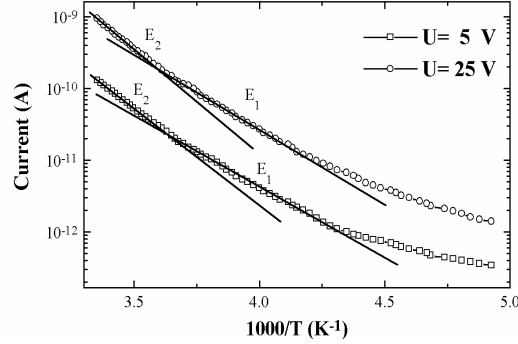
Fig. 3. $I - T$ characteristics for Si/SiO$_2$ sample ($x = 75$ %), at two applied biases [16].

4. Theoretical model

The major effect induced by the quantum confinement is that the nanocrystal surface acts like the wall of a quantum well, generating some supplementary energy levels. For semiconductors, these levels are located in the band gap. This is due to the fact that, at absolute zero, the maximum energy for the electrons is situated at the top of the valence band, so this energy value must coincide with the fundamental quantum confinement level. The simplest kind of quantum well is the rectangular one. For such wells, the comparison between the energies of the first 3 – 4 levels in an infinite quantum well and a finite one (2 – 5 eV depth) shows differences of less than 2.5 % for sizes between 1 and 10 nm [15]. This is the reason only infinite rectangular quantum wells will be considered in the following.

As shown in the previous Section, the alveolar walls of the nc-PS layer are formed by a nanowires network ensuring the carriers transport. The length/diameter ratio for the nanowires is of the order of $10^3 - 10^4$. Under such conditions, the electron Hamiltonian can be written as a sum of a longitudinal (along the wire) and a transversal parts. The longitudinal term is a one-dimensional (1D) Bloch Hamiltonian and the second one is given by a 2D infinite quantum well. The simplest description of a wire is either a square prism or a cylinder, the transversal part being modeled accordingly. Due to the diamond symmetry of the silicon, neither geometry is exact, but they both represent good first approximations. Under these conditions the electron energy is

$$E = \varepsilon_{n,k_z} + \frac{2\pi^2\hbar^2}{m^* d^2} x_{l,p}^2 = \left(\varepsilon_{n,k_z} + \frac{2\pi^2\hbar^2}{m^* d^2} x_{0,1}^2 \right) + \frac{2\pi^2\hbar^2}{m^* d^2} \left(x_{l,p}^2 - x_{0,1}^2 \right) \equiv \varepsilon_{n,k_z}^s + E_{l,p-1}. \quad (1)$$

In this equation,

$$E_{l,p} = \frac{2\pi^2\hbar^2}{m^* d^2} \left(x_{l,p+1}^2 - x_{0,1}^2 \right) \quad (2)$$

is the discrete energy level for the transversal motion and ε_{n,k_z}^s the energy of the longitudinal motion, shifted in order to have $E_{0,0} \equiv 0$. m^* is the effective mass of the electron and d the effective wire diameter (for square prism symmetry d is the square basis diagonal). For cylindrical shape, $z_{l,p} = \pi x_{l,p}$ is the p-th zero of the Bessel function $J_l(z)$, l being the orbital quantum number. In the case of a square prism, Eq. (2) becomes

$$E_{l,p} = \frac{2\pi^2\hbar^2}{m^* d^2} \left(x_{l,p+2}^2 - x_{0,2}^2 \right), \quad (2')$$

with $x_{l,p+2} = (1/2)\sqrt{l^2 + (p+2)^2}$, $p + 2 = n_x + n_y$, $l = |n_x - n_y|$, n_x and n_y being the corresponding 2D infinite square quantum well numbers. In both cases, the absence of an orbital motion means $l = 0$.

In the case of the Si/SiO$_2$ layers, one can approximate the silicon nanodots as spherical. As most of them are well under 10 nm diameter, one have no longer any proper energy band structure, but only groups of energy levels that form quasibands. Then the quantum confinement energy is also given by Eq. (2), where $z_{l,p} = \pi x_{l,p}$ is now the p-th zero of the spherical Bessel function $j_l(z)$ and again l is the orbital quantum number.

Both relations (1), (2), and (2') are valid in the effective mass approximation. Different studies [10, 11] show that this approximation is not valid in the very small size limit (under 5 nm), as the disappearance of a proper band structure would replace the effective carrier mass with the free electron one. This means the effective mass will become size-dependent [23], so that the energy will no longer be inversely proportional with the square of the diameter. However, the relations (1, 2) represent a good first approximation.

For diameters less than 5 nm, the differences between the energies of different confinement levels given by Eq. (2) are at least an order of magnitude greater than the thermal agitation energy $k_B T$, up to the room temperature. Under such conditions, the carrier concentration is given by a Boltzmann-like law, $n \propto \exp(-E_a / k_B T)$, implying a corresponding Arrhenius $I - T$ characteristic. The activation energy E_a is the absolute value of the difference between the energies of the last occupied level and the following one. When a level is practically filled (the number of independent quantum states on a level being proportional with d^2 in PS and with d^3 in Si/SiO$_2$), a following one starts to be excited and the activation energy is modified.

The ratio of the consecutive activation energies is

$$R_d = \frac{E_a''}{E_a'} = \frac{\varepsilon_{l'', p''} - \varepsilon_{l', p'}}{\varepsilon_{l', p'} - \varepsilon_{l, p}} = \frac{x_{l'', p''+1}^2 - x_{l', p'+1}^2}{x_{l', p'+1}^2 - x_{l, p+1}^2} . \tag{3}$$

The value of the ratio depends on the kind of nanocrystalline system and the excitation conditions. In the case of a nanowire, the excitation is always made from the valence band that acts as an electron reservoir, so that Eq. (3) becomes

$$R_w = \frac{x_{l'', p''+1}^2 - x_{0,1}^2}{x_{l', p'+1}^2 - x_{0,1}^2} \tag{4}$$

for cylindrical symmetry (and analogous for square one). The same thing happens for nanodots big enough to have a proper band structure. Concerning the excitation conditions, as long as one has thermal excitation only (that is low field, $eU << k_B T$), the first three levels correspond to $l = 0, 1, 2$, and $p = 0$ for cylindrical or spherical symmetries. Then R_w equals 2.29, and R_d is 2.26 for big nanodots and 1.26 for small ones. For nanowire square symmetry, the first three levels are given by ($l = 0, p = 0$), ($l = 1, p = 1$) and ($l = 0, p = 2$), and $R_w = 2.00$. If the excitation is made under a high field (i.e. $eU >> k_B T$), one has angular momentum conservation, so that for the first three levels one has $l = 0$ and $p = 0, 1, 2$. Then R_w equals 2.80 for cylindrical symmetry and 2.67 for square one, while R_d is 2.67 for big nanodots and 1.67 for small ones. If the field is applied at a temperature at which the level $l = 1, p = 0$ is already thermally excited ($p = 1$ for square nanowires), R_w is 2.25 for cylindrical and 2.09 for square nanowires, and R_d is 2.50 for big and 1.50 for small nanodots.

5. Discussion

Comparing the mean value of the activation energy for the fresh nc-PS sample, $E_m = 0.52 \pm 0.03$ eV, with the quantum confinement energy given by Eqs. (2) and (2') for ($l = 0, p = 1$), one obtains a mean diameter of 3.31 ± 0.05 nm for cylindrical symmetry and 3.63 ± 0.05 nm for square one, in good agreement with the microstructure investigations. For the stabilized samples, the first activation energy leads to a diameter of 3.22 ± 0.05 nm and 3.53 ± 0.05 nm, respectively.

The thinning of 0.1 nm is not quite plausible. However, if one takes into account the diameter dependence of the energy found in other studies (e.g. $E \propto d^{-1.02}$, see Ref. 10), the thinning would be double, i.e. practically one interatomic distance, which seems quite plausible. More than that, the ratio of the two experimental activation energies is $R_e = 2.73$, which is practically the mean value of the theoretical ratios for cylindrical and square symmetries.

These results also agree with the photon energy of the maximum observed in photoluminescence measurements. Indeed, the energy of the transition between the confinement levels ($l = 1, p = 2$) and ($l = 0, p = 1$) for the nanowire diameter found from the $I - T$ characteristic for fresh samples is $\Delta E = 1.71 \pm 0.05$ eV, approximately equal to the photon energy $E_{ph} = 1.72 \pm 0.05$ eV. The ageing blue shift from 1.72 to 1.77 eV is also in good agreement with the activation energy and diameter shifts observed from $I - T$ measurements.

The activation energies observed for Si/SiO$_2$ sample at $x = 75$ % have an experimental ratio of $R_e = 1.70$, almost equal with the theoretical value obtained for $E_a' = E_{0,1} - E_{0,0}$ and $E_a'' = E_{0,2} - E_{0,1}$ ($R_d = 1.67$). The nanodot diameter obtained from this identification is

4.48 ± 0.05 nm. This is in good agreement with the microstructure, taking into account that smaller nanodots correspond to higher resistances and so dominate the transport properties.

As the confinement level ($l = 1$, $p = 0$) is thermally excited at room temperature, one has to consider the energy of the transition between the confinement levels ($l = 2$, $p = 3$) and ($l = 1$, $p = 0$) for the comparison with the photon energy of the maximum observed in photoluminescence measurements. For the nanodot diameter found from the $I - T$ characteristic, this energy is 1.67 ± 0.05 eV, in good agreement with the experimental value $E_{ph} = 1.70 \pm 0.05$ eV.

6. Conclusions

From current – temperature characteristics one can observe that the quantum confinement controls the bulk (inside the nanocrystals) excitation processes for both nc-PS and Si/SiO$_2$ nanocomposites. While the $I - T$ curves for Si/SiO$_2$ nanocomposites present two activation energies, those for nc-PS show only one energy for fresh samples. The second one appears for oxidized samples, where the nanowires are thinned.

The model permits to identify the activation energies as differences between quantum confinement levels, on the basis of the consecutive activation energies ratio. Besides, the model allows the evaluation of the nanocrystallites diameter. The obtained values are in good agreement with the microstructure results for both nc-PS and Si/SiO$_2$ nanocomposites.

The photon energy corresponding to the maxima observed in photoluminescence measurements for each material can also be related to transitions between quantum confinement levels.

Acknowledgements

References

[1] T. V. Torchynska, J. Appl. Phys. **92**, 4019 (2002).
[2] R. J. Walters, G. I. Bourianoff, H. A. Atwater, Nature Mater. - Adv. Online Public. doi: 10.1038/nmat 1307 (2005).
[3] G. D. J. Smit, S. Rogge, T. M. Klapwijk, Appl. Phys. Lett. **81**, 3852 (2002).
[4] M. Ben-Chorin, F. Möller, F. Koch, Phys. Rev. B **49**, 2981 (1994).
[5] V. Ioannou-Sougleridis, T. Ouisse, A. G. Nassiopoulou, F. Bassani, F. Arnaud d'Avitaya, J. Appl. Phys. **89**, 610 (2001).
[6] M. L. Ciurea, M. Draghici, V. Iancu, M. Reshotko, I. Balberg, J. Luminesc. **102-103**, 492 (2003).
[7] V. Iancu, M. Draghici, L. Jdira, M. L. Ciurea, J. Optoelectron. Adv. Mater. **6**, 53 (2004).
[8] D. M. Pooley, H. Ahmed, H. Mizuta, K. Nakazato, J. Appl. Phys. **90**, 4772 (2001).
[9] M. Ben-Chorin, F. Möller, F. Koch, Phys. Rev. B **51**, 2199 (1995).
[10] C. Delerue, G. Allan, M. Lannoo, Phys. Rev. B **48**, 11024 (1993).
[11] J. Heitmann, F. Müller, L. X. Yi, M. Zacharias, D. Kovalev, F. Eichhorn, Phys. Rev. B **69**, 195309 (2004).
[12] Y. L. He, X. N. Liu, Z. C. Wang, G. X. Cheng, L. C. Wang, S. D. Yu, Sci. China Ser. A **36**, 248 (1993).
[13] G. Y. Hu, R. F. O'Connell, Y. L. He, M. B. Yu, J. Appl. Phys. **78**, 3945 (1995).
[14] Y. L. He, Y. Y. Wei, G. Z. Zhang, M. B. Yu, M. Liu, J. Appl. Phys. **82**, 3408 (1997).
[15] M. L. Ciurea, I. Baltog, M. Lazar, V. Iancu, S. Lazanu, E. Pentia, Thin Solid Films **325**, 271 (1998).
[16] V. Iancu, L. Jdira, M. Draghici, M. R. Mitroi, I. Balberg, M. L. Ciurea, Proc. IEEE CN 03TH8676, Int. Semicond. Conf. CAS 2003, Sinaia, 3 – 6 octombrie 2003, **1**, 83 (2003).
[17] D. Kovalev, H. Heckler, G. Polisski, F. Koch, Phys. Status Solidi (b) **215**, 871 (1999).
[18] M. L. Ciurea, E. Pentia, A. Manea, A. Belu-Marian, I. Baltog, Phys. Stat. Sol. (b) **195**, 637 (1996).
[19] M. L. Ciurea, V. Iancu, V. S. Teodorescu, L. C. Nistor, M. G. Blanchin, J. Electrochem. Soc. **146**, 3516 (1999).
[20] V. S. Teodorescu, L. C. Nistor, M. G. Blanchin, V. Iancu, M. Draghici, M. L. Ciurea, Proc. IEEE CN 99TH8389 Int. Semicond. Conf. CAS '99, **1**, 101 (1999).
[21] V. S. Teodorescu, M. L. Ciurea, V. Iancu, M. G. Blanchin, Proc. IEEE CN 04TH8748, Int. Semicond. Conf. CAS 2004, Sinaia, 3 – 6 octombrie 2004, **1**, 59 (2004).
[22] M. Dovrat, Y. Goshen, J. Jedrzejewski, I. Balberg, A. Sa'ar, Phys. Rev. B **69**, 155311 (2004).
[23] J. Wang, A. Rahman, A. Ghosh, G. Klimeck, M. Lundstrom, http://arxiv.org/ftp/cond-mat/papers/0412/0412278.pdf (2004).